Available online at www.sciencedirect.com

ScienceDirect

Procedia Engineering 199 (2017) 3474–3479

Procedia Engineering

www.elsevier.com/locate/procedia

X International Conference on Structural Dynamics, EURODYN 2017

FLuttering Energy Harvester for Autonomous Powering (FLEHAP): aeroelastic characterisation and preliminary performance evaluation

Stefano Olivieri[a,*], Gregorio Boccalero[b,c], Andrea Mazzino[a,d], Corrado Boragno[b]

[a]*DICCA, Dipartimento di Ingegneria Civile, Chimica e Ambientale, Via Montallegro 1, 16145 Genova, Università degli Studi di Genova, Italy*
[b]*DIFI, Dipartimento di Fisica, Via Dodecaneso 33, 16146, Genova, Università degli Studi di Genova, Italy*
[c]*DCCI, Dipartimento di Chimica e Chimica Industriale, Via Dodecaneso 33, 16146, Genova, Università degli Studi di Genova, Italy*
[d]*Consorzio CINFAI and INFN, Sezione di Genova, Via Montallegro 1, Genova, 16145, Italy*

Abstract

Significant efforts are being devoted in order to develop efficient and reliable energy harvesters based on interactions between structures and environmental fluid flows such as wind or marine currents. In this framework, a fully-passive energy harvester of centimetric size employing an elastically bounded wing has been developed. The system exploits the coupled-mode flutter, leading in certain conditions to finite amplitude and self-sustained oscillations. Electrical output power levels up to 15[mW] have been reached by an experimental prototype within a wind range between 2 and 5 [m/s] by means of electromagnetic coupling as the conversion strategy. Focusing on the aeroelastic point of view, it is crucial to investigate how the kinematics (i.e. flapping amplitude and frequency, phase between the pitch and plunge motion DoFs) varies with the main parameters (e.g. wind velocity and wing geometry), in order to identify the optimal conditions for potential harvesting. With this goal in mind, we present and discuss the results for a representative configuration of the device (first without the extraction mechanism), exploring the behavior within the design wind range, combining wind-tunnel experiments, three-dimensional CFD simulations and the development of a quasi-steady phenomenological model. We find that both the amplitude and the frequency of the flapping motion are maximised for a certain wind velocity. Moreover, the phase between pitch and plunge changes abruptly when close to this condition. Hence, we estimate the mechanical power that the wing is able to collect and the Betz efficiency, e.g. the ratio between the latter and the power available in the flow. The mathematical model is then enriched by additional terms mimicking an electrical resistive circuit and predictions are made regarding the extracted power and global efficiency of the system, showing the presence of optimal conditions for which these quantities are maximised. Finally, we outline future challenges in the harvester development towards a realistic deployment.

© 2017 The Authors. Published by Elsevier Ltd.
Peer-review under responsibility of the organizing committee of EURODYN 2017.

Keywords: energy harvesting; fluid-structure interactions; electromagnetic-coupling; computational fluid dynamics; limit-cycle oscillations; quasi-steady phenomenological model;

* Corresponding author. Tel.: +39-010-353-2560 ; Fax.: +39-010-353-2546.
E-mail address: stefano.olivieri@edu.unige.it

1877-7058 © 2017 The Authors. Published by Elsevier Ltd.
Peer-review under responsibility of the organizing committee of EURODYN 2017.
10.1016/j.proeng.2017.09.456

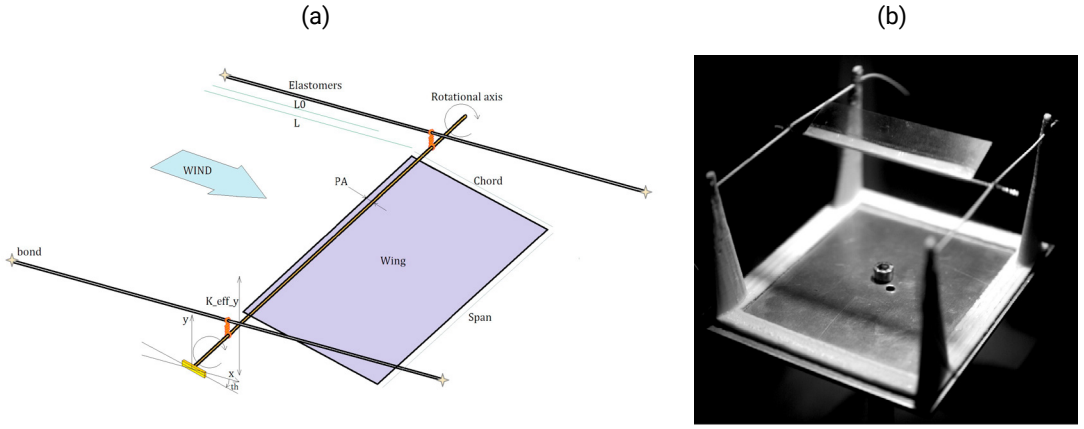

Fig. 1. The FLEHAP system (without energy extraction apparatus) in the configuration chosen for the present investigation, in (a) sketch and (b) experimental realization.

1. Introduction

In the last decades, fluid-structure interactions (FSI) have deserved attention not only for design issues related to prevent failures, but also for energy harvesting purposes [1,2,3], with the challenge in developing efficient and reliable devices exploiting aeroelastic instabilities (e.g.: flutter, galloping, vortex-induced vibrations), where typically finite-size oscillations are sought on purpose and the associated mechanical power is converted into electrical one [4]. This kind of systems are conceived to exploit either the interaction with environmental currents, such as wind or in water, and with internal flows in man-made ambients, with the main goal of supplying wireless sensor networks related to the Internet of Things [5].

In this framework, this contribution concerns a novel device based on an elastically bounded wing exploiting the coupled-mode flutter aeroelastic instability [6,7,8,9,10]. The device is under active development and has been named FLEHAP ("FLuttering Energy Harvester for Autonomous Powering"). Fig. 1 depicts the system in its essential form: the wing is made by a polyvinyl acetate foil glued to a brass rod (pivot axis). This latter is connected to four elastomers so that it can rotate freely. The resulting motion degrees of freedom are three, i.e. vertical translation (plunge), rotation around the pivot axis (pitch) and horizontal translation. The system is completely passive and the constructive layout is rather simple with a potential benefit from the cost viewpoint.

When invested by an incompressible flow and if the physical parameters are in a proper range, regular and self-sustained limit cycle oscillations (LCOs) occur: the pivot point (i.e. the trace of the pivot axis in a lateral view) undergoes a substantially vertical harmonic motion while the wing performs a flapping movement, with periodic stretching and relaxing of the elastomers. Output power levels up to 15[mW] have been reached by an experimental prototype for a wind range between 2 and 5 [m/s] by means of an electromagnetic coupling extraction method. For a detailed description regarding the proper application and the experimental development, the reader can refer to [9,10].

Previous work [10,7] has been devoted to identify the threshold condition for sustained flapping (i.e. to determine the cut-in flow speed). However, the characterisation of the nonlinear regime above this threshold has not been fully addressed, yet it is crucial in order to identify the optimal conditions for potential harvesting. In this work, we seek to characterise the flapping kinematics for a representative configuration, by combining wind-tunnel experiments, numerical simulations and an analytical description based on a quasi-steady phenomenological model, both for increasing our physical understanding of this aeroelastic system and estimating the available mechanical power for energy extraction. Related to the latter point, we proceed further by employing the quasi-steady model taking into account also the extraction stage in order to provide a preliminary performance evaluation (i.e. output power, efficiency).

2. Methods

For our investigation, we choose the following configuration (see Fig. 1a): wing made by a rectangular plate with chord $c = 20$[mm], span $s = 70$[mm], thickness $\delta = 100[\mu$m]; pivot axis located at 0.5[mm] from the leading edge, total mass of the moving system $m = 0.845$[g], elastomer diameter $D_0 = 1.2$[mm] and length $l_0 = 47.3$[mm], at rest; a pre-stretching is given so that the initial length is $L = 66.3$[mm]. The elastic force magnitude for each elastomer is thus given by $|F_{\rm el}| = GA_0(L/l_0 - (l_0/L)^2)$ [11], where the material shear modulus value is $G = 0.534$[MPa] and $A_0 = \pi D_0^2/4$. The natural frequency of the system relative to the vertical motion can be measured from the free oscillation of the pivot point when perturbating the elastically bounded wing along the vertical direction, in still fluid, having $f_{\rm n}^{(y)} = 13.2$[Hz]. From this quantity, combined with the given mass, we can define an equivalent linear stiffness $\mathcal{K}_{(y)}^{\rm eff}$. In the following we briefly give the main information concerning the three and complementary approaches for our study.

2.1. Experimental setup

Our measurements are performed using a subsonic, aspirating, open-circuit wind tunnel built at the Physics Department of the University of Genoa, whose constructive and operational details are described in [10]. The device shown in Fig. 1b is posed approximately at the center of the test camera and the wing motion is recorded by a high-definition camera at 500 [fps]; from the video analysis, we collect the trajectory of the pivot point (PP), the trailing edge (TE) and the wing angle respect to horizontal line.

2.2. Computational fluid dynamics

Numerical simulations are performed using the open source toolkit *OpenFOAM*® [12]. The basic setup regarding the mathematical model and solvers is the same as in [10]. Here, however, we perform three-dimensional simulations and restraints follow the nonlinear elastomeric law given at the beginning of Sec. 2. The wing is represented by a 3-D plate with rectangular cross-section inside a domain box, with same dimensions as the experimental test chamber. The hexahedral-based used mesh counts 462620 cells with resolution varying through several refinement levels from 0.02 (at the box boundaries) to 10^{-3} [m] (at the wing surface).

2.3. Quasi-steady phenomenological model

We seek for an analytical description of the system by means of a quasi-steady phenomenological model originally proposed for falling plates [13]. By considering a reference frame that is co-rotating with the wing, the dynamic governing equations are:

$$(m + m_{11})\,\dot{v}_{x'} = (m + m_{22})\,\dot{\theta}\,v_{y'} + F_{x'}^{el} - m'g\sin\theta - \rho_{\rm f}\Gamma\tilde{v}_{y'} - F_{x'}^{\nu} + F_{x'}^{\rm EC} \tag{1}$$

$$(m + m_{22})\,\dot{v}_{y'} = -(m + m_{11})\,\dot{\theta}\,v_{x'} + F_{y'}^{el} - m'g\cos\theta + \rho_{\rm f}\Gamma\tilde{v}_{x'} - F_{y'}^{\nu} + F_{y'}^{\rm EC} \tag{2}$$

$$(I_G + I_a)\,\dot{\omega} = (m_{11} - m_{22})\,v_{x'}\,v_{y'} + \tau^{el} - \tau^{\nu} - l_\tau\rho_{\rm f}\Gamma\tilde{v}_{x'} + \tau^{\rm EC} \tag{3}$$

together with $\dot{x}'_G = v_{x'} + \omega\,y'_G$, $\dot{y}'_G = v_{y'} - \omega\,x'_G$ and $\dot{\theta} = \omega$. Here, $v_{x'}$ and $v_{y'}$ are the center of mass velocity components, $\tilde{v}_{x'} = (v_{x'} - U\cos\theta)$ and $\tilde{v}_{y'} = (v_{y'} + U\sin\theta)$ are those relative to the unperturbed flow, $m_{\rm f} = \rho_{\rm f}cs\delta$, $m' = m - m_{\rm f}$, I_G is the moment of inertia with respect to the center of mass G, x'_G and y'_G are the coordinates of the latter, θ is the pitching angle, $\mathbf{F}^{\rm el}$ is the elastic force and $l_\tau = c(3-\cos(\theta)/2)/4$ is the moment arm of the circulatory force. The added mass quantities m_{11}, m_{22} are expressed for the plate of rectangular cross-section following [14]: $m_{11} = (3\pi/8)\rho_{\rm f}\delta^2$, $m_{22} = (3\pi/8)\rho_{\rm f}c^2$, while $I_{\rm a} = (5\pi/256)\rho_{\rm f}(c^2 - \delta^2)^2 + m_{22}r_O^2$ according to Bryant *et al.* [15]. The expressions for the aerodynamic quantities, i.e. the circulation Γ, the viscous force $\mathbf{F}^{\nu}$ and the dissipative fluid torque τ^{ν}, are based on those of Ref. 13 and make use of several free parameters: C_T and C_R are the translational and rotational lift coefficients, respectively, C_D^0 and $C_D^{\pi/2}$ are the drag coefficients while C_τ is the dissipative torque coefficient. After a calibration against the experimental data, the following values were chosen: $C_T = 2.1$, $C_R = 1.5$, $C_D^0 = 0.1$, $C_D^{\pi/2} = 8.0$ and $C_\tau = 8.25$. Finally, equations (1–3) contain a simple extraction term, mimicking the effect of a purely resistive circuit by using a linear relation between the generated electromotive force and the pivot point velocity similar to [16].

3. Results

3.1. Flapping kinematics

In the present section, we present and discuss our findings measured/computed with the three methods introduced in the previous section, starting from the flapping kinematics. Fig. 2 shows the trajectories from a side view (x-y plane) of pivot point (PP) and trailing edge (TE) while Fig. 3 reports the frequency, amplitude and phase (between pitch and plunge), as a function of the wind speed. Overall, results look in good agreement: regular flapping motion is found for all cases in each investigation, with finite-size amplitude, an essentially vertical motion of the PP and a lemniscate-like shape for the TE trajectory.

Looking at the experimental results in Fig. 3, from the lowest flow speed (2.5[m/s]), both frequency and amplitude of flapping increase while increasing U up to 4[m/s] where they suddenly reach a peak. For $U > 4$ [m/s], the phase between pitch and plunge increases abruptly to a value close to 90[deg] and the resulting shapes of the trajectory change, showing a wider amplitude of the TE oscillation and the opposite trend for the PP. Displacements are typically of the same order of the wing chord and a maximum exists for the PP amplitude (which is a quantity of interest for energy harvesting). In this regard, as evident while looking at Fig. 3b, a notable difference is found between the the experimental values and the prediction by CFD which anticipates and underestimates this condition. We ascribe this discrepancy to several possible causes (e.g.: constructive details, non-uniformity of the real incoming flow) and plan future studies in order to improve the quantitative agreement. The phenomenological model, on the other

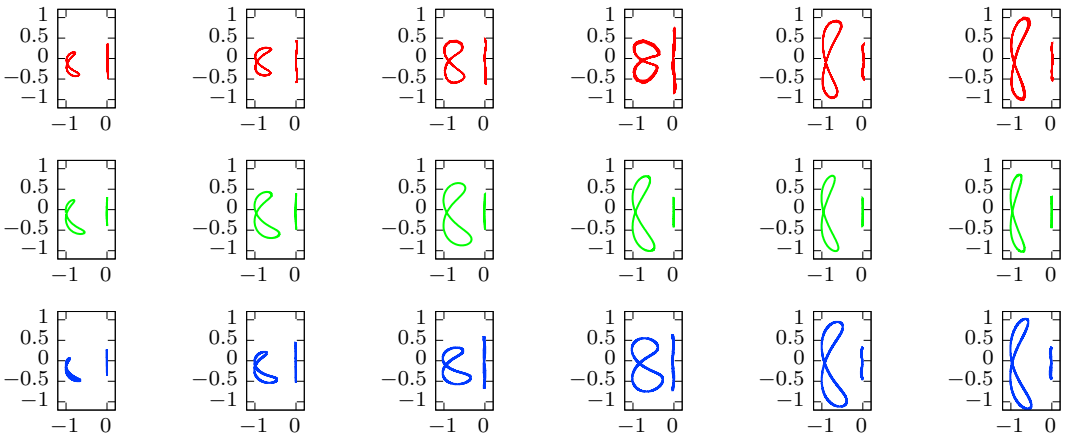

Fig. 2. Pivot point and trailing edge trajectories in the x-y plane from experiments (first row), CFD simulations (second row) and phenomenological model (third row), for wind speed $U = (2.5, 3.0, 3.5, 4.0, 4.5, 5.0)$ [m/s] (from left to right). Lengths are normalized with the wing chord c.

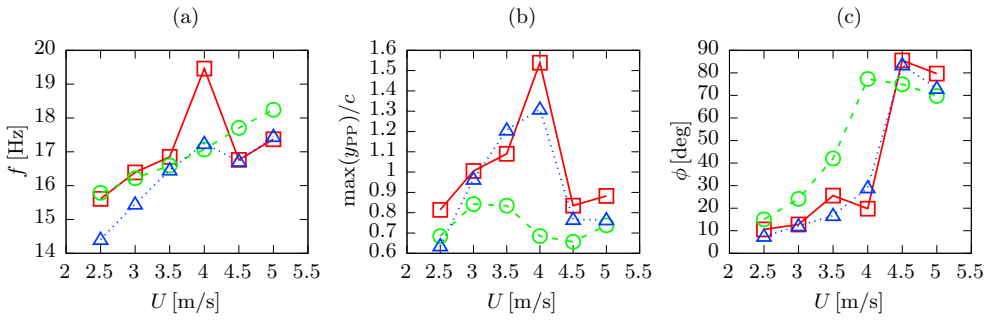

Fig. 3. Flapping (a) frequency, (b) amplitude (normalized with the wing chord) and (c) phase between pitch and plunge, from experiments (squares, filled line), CFD simulations (circles, dashed line) and phenomenological model (triangles, dotted line).

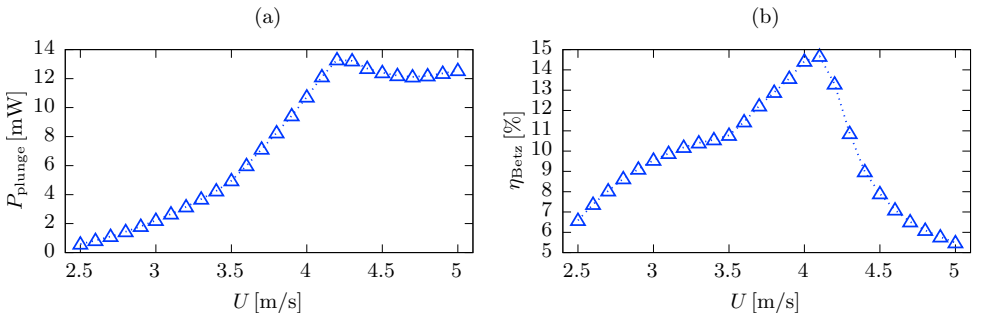

Fig. 4. Estimation by the phenomenological model: (a) mechanical power trasferred from the flow to the flapping wing; (b) Betz efficiency.

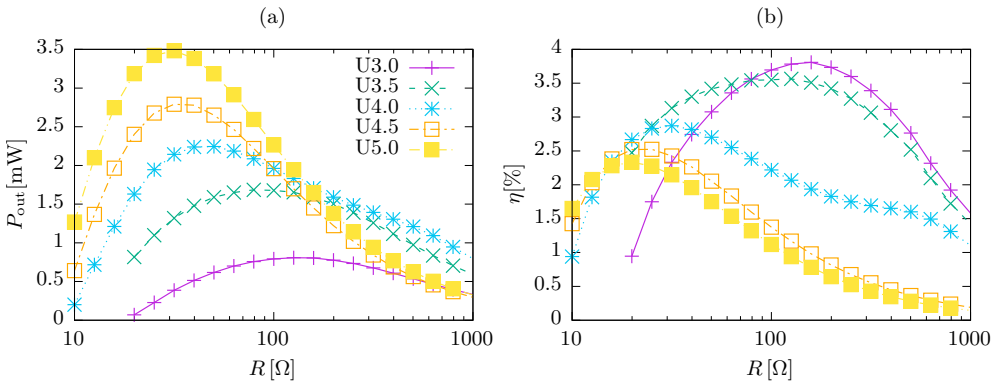

Fig. 5. Phenomenological model's prediction of (a) electrical power harvested by the system and (b) global efficiency, as a function of the applied resistive load and for different wind speeds.

hand, provides values which are closer to the experimental ones, both in frequency, amplitude and phase. The peak appearing for $U = 4\,[\text{m/s}]$ is however still smoothed with respect to the experimental evidence. It has to be noted that the model might not properly reproduce some unsteady, time-history dependent features [13]. Despite this and the semi-empirical nature which limits the general applicability without calibration, the relatively simple analytical description given by this tool may aid in the design of the device.

3.2. Power extraction

Following the latter point, as a further step we employ the phenomenological model to estimate the energy harvesting potential of the system, starting by computing the mean mechanical power transferred to the moving wing, considering in particular the one associated to the plunge motion, i.e.: $P_{\text{plunge}} = \frac{1}{T}\int_t^{t+T} L\,\dot{y}_{\text{PP}}\,\mathrm{d}\tilde{t}$ where L is the lift force and $\dot{y}_{\text{PP}}$ is the pivot point vertical velocity component. Moreover, we are interested in the Betz efficiency, defined as: $\eta_{\text{Betz}} = P_{\text{plunge}}/\frac{1}{2}\rho_{\text{f}}U^3 sd$ where d is the maximum vertical displacement swept by the wing. Both quantities are reported in Fig. 4. We observe that the plunge power (Fig. 4a) first increases with the wind speed until a maximum value for $U \approx 4.25[\text{m/s}]$, slightly decreasing for larger values. The Betz efficiency (Fig. 4b), on the other hand, shows a maximum for $U \approx 4[\text{m/s}]$, with a sharp drop when increasing the flow speed. Therefore, the previously discussed transitional condition turns out to be crucial also from the power extraction viewpoint.

Subsequently, the extraction term in the model is activated and a parametric study is performed, for different flow velocities and varying the applied resistive load. Now an electrical output power is obtained, its mean value being defined as $P_{\text{out}} = V_{\text{rms}}^2/R$, together with the global efficiency $\eta = P_{\text{out}}/\frac{1}{2}\rho_{\text{f}}U^3 sd$. Results of the analysis are presented in Fig. 5: smooth power curves showing the existence of optimal loads, for each velocity, that maximise the output power and the global efficiency. For the first quantity (Fig. 5a), the optimal load gets higher when decreasing U. The

corresponding power maximum value always grows with U; this should not be intended in disagreement with the plunge power curve shown in Fig. 4a, since in presence of extraction the flapping kinematics gets altered and typically damped. Concerning the global efficiency (Fig. 5b), both the maximum value and the corresponding optimal load decrease when increasing U (with the second being slightly different compared to that for maximum power). The present study therefore evidences the possible need of a trade-off between effective and efficient performance.

4. Conclusions

The present work aimed at improving the comprehension of a particular aeroelastic system composed by a moving rigid wing bounded through elastomeric elements and suitable for energy harvesting purposes, focusing on the analysis of the nonlinear flapping regime by combining wind tunnel experiments, CFD simulations and a quasi-steady phenomenological model. The main finding is that an optimal condition at an intermediate wind speed exists where the fluid-structure interaction is maximised both in terms of frequency and amplitude of the flapping motion. Furthermore, a prediction of the extractive performance has been given using the quasi-steady model.

Nevertheless, several points still require to be addressed in a further detailed way, such as a deeper comprehension of the optimal (transitional) condition on physical arguments and its dependence upon other parameters ruling the system dynamics. On the other hand, improved CFD simulations in closer agreement with experimental results would allow a complementary analysis of the existing data and a reliable testing of other configurations towards the system optimisation.

Acknowledgements

This article is based upon work from COST Action MP1305, supported by COST (European Cooperation in Science and Technology). We thank the financial support from the PRIN 2012 project n. D38C13000610001 funded by the Italian Ministry of Education. AM is also grateful for the financial support for the computational infrastructure from the Italian flagship project RITMARE.

References

[1] A. Abdelkefi, Aeroelastic energy harvesting: A review, Int. J. Eng. Sci. 100 (2016) 112 – 135.
[2] J. McCarthy, S. Watkins, A. Deivasigamani, S. John, Fluttering energy harvesters in the wind: A review, J. Sound Vib. 361 (2016) 355 – 377.
[3] J. Young, J. Lai, M. F. Platzer, A review of progress and challenges in flapping foil power generation, Prog. Aerosp. Sci. 67 (2014) 2–28.
[4] J. A. C. Dias, C. De Marqui, A. Erturk, Hybrid piezoelectric-inductive flow energy harvesting and dimensionless electroaeroelastic analysis for scaling, Appl. Phys. Lett. 102 (2013) 044101.
[5] J. Gubbi, R. Buyya, S. Marusic, M. Palaniswami, Internet of things (IoT): A vision, architectural elements, and future directions, Future Gener. Comput. Syst. 29 (2013) 1645–1660.
[6] C. Boragno, R. Festa, A. Mazzino, Elastically bounded flapping wing for energy harvesting, Appl. Phys. Lett. 100 (2012) 253906.
[7] A. Orchini, A. Mazzino, J. Guerrero, R. Festa, C. Boragno, Flapping states of an elastically anchored plate in a uniform flow with applications to energy harvesting by fluid-structure interaction, Phys. Fluids 25 (2013) 097105.
[8] C. Boragno, G. Boccalero, A new energy harvester for fluids in motion, Proc. SPIE 9431 (2015) 94310G–94310G–6.
[9] G. Boccalero, C. Boragno, D. D. Caviglia, R. Morasso, FLEHAP: A Wind Powered Supply for Autonomous Sensor Nodes, J. Sens. Actuator Netw. 5 (2016) 15.
[10] S. Olivieri, G. Boccalero, A. Mazzino, C. Boragno, Fluttering conditions of an energy harvester for autonomous powering, Renew. Energ. 105 (2017) 530 – 538.
[11] S. L. Rosen, Fundamental principles of polymeric materials, Wiley, 1982.
[12] OpenFOAM. The Open Source CFD Toolbox. User Guide, 2015. URL: `http://www.openfoam.org`.
[13] A. Andersen, U. Pesavento, Z. J. Wang, Unsteady aerodynamics of fluttering and tumbling plates, J. Fluid Mech. 541 (2005) 65–90.
[14] W. Huang, H. Liu, F. Wang, J. Wu, H. P. Zhang, Experimetal study of a freely falling plate with an inhomogeneous mass distribution, Phys. Rev. E 88 (2013) 053008.
[15] M. Bryant, J. C. Gomez, E. Garcia, Reduced-order aerodynamic modeling of flapping wing energy harvesting at low Reynolds number, AIAA J. 51 (2013) 2771–2782.
[16] H. Dai, A. Abdelkefi, U. Javed, L. Wang, Modeling and performance of electromagnetic energy harvesting from galloping oscillations, Smart Mater. Struct. 24 (2015) 045012.